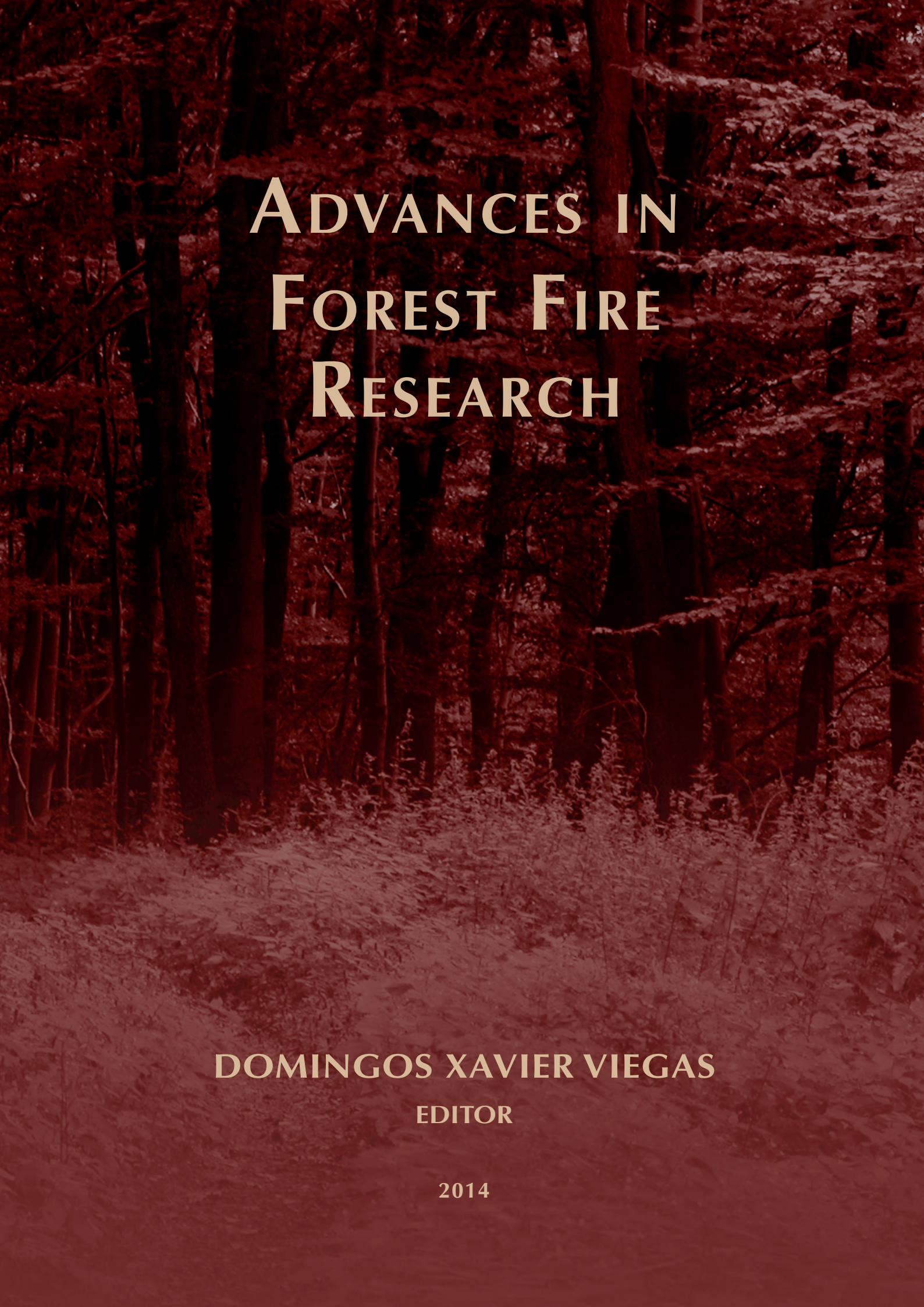

Advances in Forest Fire Research

DOMINGOS XAVIER VIEGAS

EDITOR

2014

Overview of the 2013 FireFlux-II Grass Fire Field Experiment

CB Clements[a], B Davis[a], D Seto[a], J Contezac[a], A Kochanski[b], J-B Fillipi[c], N Lareau[a], B Barboni[c], B Butler[d], S Krueger[b], R Ottmar[e], R Vihnanek[e], W E Heilman[f], J Flynn[g], M A Jenkins[b], J Mandel[h], C Teske[i], D Jimenez[d], J O'Brien[j], and B. Lefer[g]

[a] *Fire Weather Research Laboratory, Department of Meteorology and Climate Science, San José State University, San José, CA, USA.* craig.clements@sjsu.edu
[b] *Department of Atmospheric Sciences, University of Utah, UT, USA*
[c] *University of Corsica, Corsica, France*
[d] *Fire Sciences Laboratory, Missoula, MT, USA*
[e] *Pacific Northwest Wildland Fire Sciences Laboratory, WA, USA*
[f] *USFS, Northern Research Station, Lansing, MI, USA*
[g] *University of Houston, Houston, TX USA*
[h] *University of Colorado, CO, USA*
[I] *University of Montana, MT, USA*
[j] *USFS Southern Research Station, GA USA*

Abstract

In order to better understand the dynamics of fire-atmosphere interactions and the role of micrometeorology on fire behaviour the FireFlux campaign was conducted in 2006 on a coastal tall-grass prairie in southeast Texas, USA. The FireFlux campaign dataset has become the international standard for evaluating coupled fire-atmosphere model systems. While FireFlux is one of the most comprehensive field campaigns to date, the dataset does have some major limitations especially the lack of sufficient measurements of fire spread and fire behaviour properties. In order to overcome this, a new, more comprehensive field experiment, called FireFlux II, was conducted on 30 January 2013. This paper will address the experimental design and preliminary results. The experiment was designed to allow an intense head fire to burn directly through an extensive instrumentation array including fixed 42-m and three 10-m micrometeorological towers (Figure 2). The fuels consist of a mixture of native grasses.Each tower was equipped with a variety of sensors, including 3D sonic anemometers, pressure sensors, heat flux radiometers, and an array of fine-wire thermocouples to measure plume temperatures. The experiment was carried out under red flag warning conditions with strong winds of 8 m s-1 and relative humidity of approximately 24%. Instrumentation also included a scanning Doppler wind lidar, microwave temperature profiler, radiosonde balloons for upper-air soundings, a full suite of air quality instrumentation located downwind, and multiple ground and tower mounted infrared and visible video cameras. In addition, the fire spread was monitored from the air using helicopter mounted infrared and visible video cameras. Because the experiment was designed to be conducted under a north wind, the timing of the experimental period only allowed for a northwest wind. This required the instrumentation array to be moved in order to document the fire spread and was a limitation to the experiment. Preliminary results showed that the fire spread rate was ~1.5-2.5 m s-1 for the head fire while the flanks spread at 0.7 m s-1. The surface pressure field indicated that a low-pressure region formed downwind of the advancing fire front. The observations from the 42-m tower show that the strongest fire-induced winds occur a the surface in the cross-wind direction.

Keywords*: Grass fire, field experiment, fire-atmosphere interactions, micrometeorology, fire-induced winds*

1. Introduction

Studies on the fine-scale structure of fire-atmosphere interactions and fire behaviour have been based mostly on numerical simulations using coupled fire-atmosphere models (Clark *et al*. 1996; Mell *et al*. 2009; Linn and Cunningham 2005; Kochanski *et al*. 2013; Fillipi *et al*. 2013) and few field campaigns (Cheney *et al*. 1999; Clements *et al*. 2007). To better understand the dynamics of fire-atmosphere

interactions and the role of micrometeorology on fire behaviour, the FireFlux campaign was conducted in 2006 on a coastal tall-grass prairie in southeast Texas, USA (Clements *et al*. 2007, 2008). The FireFlux campaign dataset has become an international standard for evaluating coupled fire-atmosphere model systems. While FireFlux is one of the most comprehensive field campaigns to date, the dataset does have major limitations, especially the lack of sufficient measurements of fire spread and fire behaviour properties. In order to overcome these limitations, a new and more comprehensive field experiment, called FireFlux II, was conducted on 30 January 2013. This paper will address the experimental design and preliminary results.

2. Experimental Design and Instruments

The FireFlux II (FF2) field campaign was conducted at same plot as FireFlux at the University of Houston Coastal Center in Texas, USA, on 30 January 2013. The experiment was designed to allow for an intense head fire to burn directly through an extensive instrumentation array that included four meteorological towers, one fixed 42-m tower and three 10-m towers (Figure 1). The towers were equipped with a variety of sensors (Table 1), including three-dimensional sonic anemometers, pressure sensors, heat flux radiometers, and an array of fine-wire thermocouples to measure plume temperatures. Also located within the prairie were two interspersed grids of 28 surface thermocouples, buried underground, 18 pressure sensors positioned ~3.0 m above the burn plot, and 8 fire behaviour sensor packages that measured flame temperature, heat fluxes and gas velocities ~1 m AGL.
A key platform and instrumentation suite deployed during FF2 was the California State University-Mobile Atmospheric Profiling System (CSU-MAPS) (Clements and Oliphant 2014). The CSU-MAPS includes a truck mounted scanning Doppler wind lidar and a microwave profiling radiometer used to continuously measure background and plume thermodynamic and kinematic properties throughout the experimental period. The Doppler lidar provided high-resolution measurements of smoke plume aerosol backscatter intensity and radial wind velocities across the plot and around the fire front. The lidar has a range gate resolution of 18 m and the temperature profiler has a vertical resolution that scales with height, with a finer resolution of 50 m within the boundary layer. The CSU-MAPS also includes a mobile, trailer-mounted 32 m meteorological tower that is equipped with 5 levels of 2-d sonic anemometers and thermistor/hygristor sensors. In addition, a radiosonde system was used for an in-situ upper-air sounding taken just before ignition. Emissions and air chemistry were measured with a full suite of gas and particle samplers located downwind of the experimental plot (Figure 1). Multiple ground and tower mounted infrared and visible video cameras were used for measuring fire behaviour properties. In addition, the fire spread was monitored from the air using helicopter mounted infrared and visible video cameras. Table 1 provides a detailed description of meteorological instruments used during the experiment.

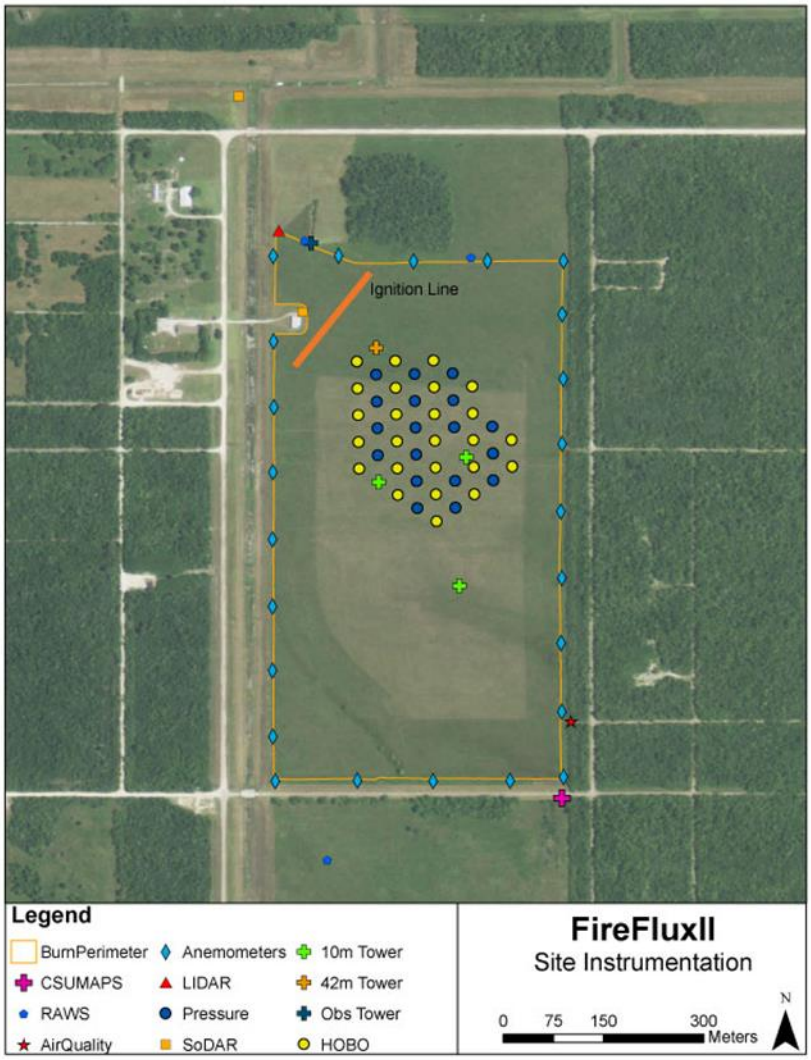

Figure 1. A map of the experimental setup during FireFlux II conducted on 30 Jan 2013.

2.1. Site description

The experimental plot was a natural tall-grass, of 155 acres (0.63 km^2) in size. The fuels consisted of a mixture of native grasses, including big bluestem (*Andropogon gerardi*), little bluestem (*Schizachyrium scoparium*), and long spike tridens (*Tridens strictus*). Fuel loading calculations were made from 20 destructive sampling plots. The average fuel loading for the experimental unit was 2.88 tons $acre^{-1}$.

The experiment was to be conducted under a north wind. However, synoptic conditions, as well as the timing of the experimental period, only allowed for a northwest wind as the best scenario. The decision was made to take advantage of the lesser than ideal conditions. WRF-SFire simulations (Mandel *et al*. 2012, Kochanski *et al*. 2013) were conducted to confirm the idealized fire spread under a northwest wind and based on these simulations, the instrumentation array was reconfigured just 24 hours prior to ignition. The reconfiguration was aimed to provide the most efficient experimental configuration for capturing the expected fire spread and maximize the number of instruments in the path of the fire.

2.2. Fuel moistures

Fuel moisture calculations were made from 20 different sampling plots. Three different sample types were collected 30 minutes prior to ignition: upper level grass (UL), lower level grass (LL), and forb (a herbaceous flowering plant). The boundary between the two grass layers was assessed based on the visual center of the mass height of the grass. Table 2 describes the moisture content percentages in detail.

3. Preliminary Results

3.1. Synoptic environment

The ignition occurred at 15:04 (CST) local time on 30 January 2013 and was associated with a post-frontal environment. The month of January was associated with above average precipitation and weak frontal systems, limiting ideal experimental conditions that required strong post-frontal northerly winds. Due to the excessive rain, soil conditions were wet with some regions of standing water within the experimental plot. A cold frontal passage the previous night created a strong northwesterly surface flow in excess of 8 m s-1, with gusts up to 12 m s-1, as well as a relative humidity of approximately 24% at the time of ignition (Figure 2). These conditions led to a red flag warning to be issued by the National Weather Service for the day of the experiment. A radiosonde launched 40 minutes prior to the ignition shows that the daytime boundary layer associated with a shallow superadiabatic surface layer and nearly adiabatic to slightly stable above the surface layer up to a capping inversion at nearly 2000 m aloft. The upper-level winds transition to strong westerly flow from the more northwesterly at the surface (Figure 3).

3.2. Preliminary spread analysis

The fire quickly spread from its ignition to the southeast side of the plot in 4 min while the flank continued to spread to the south end of the experimental plot. Using the ground based temperature loggers (Fig 4) to determine the fire front position, the fire spread rate was calculated to be ~1.5-2.5 m s^{-1} for the head fire while the flanks spread at 0.7 m s^{-1}.

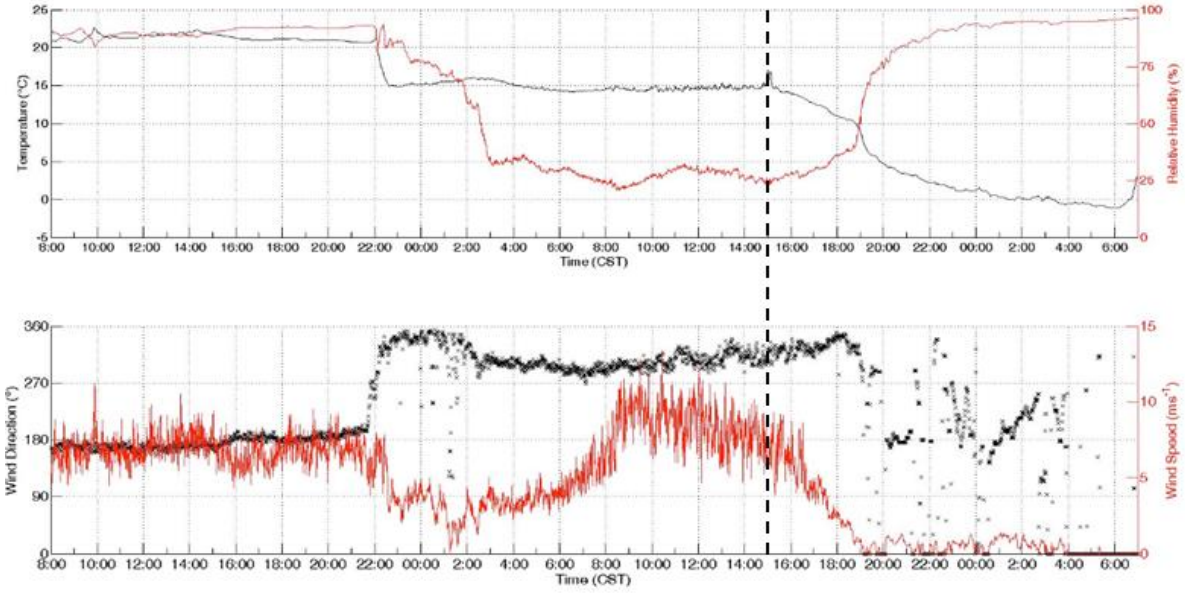

Figure 2. Surface conditions before, during, and after the burn, January 29-30, 2013. Ignition time is marked by the vertical dashed line.

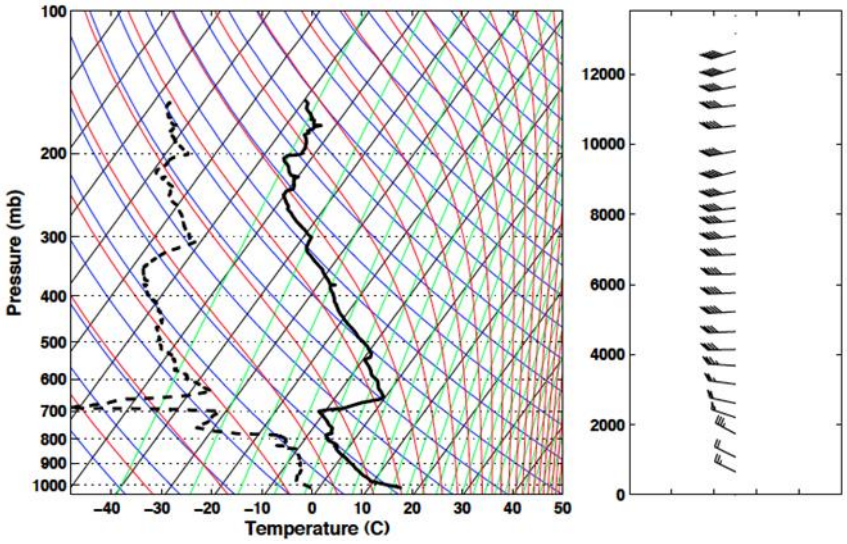

Figure 3. Skew-T diagram of radiosonde sounding taken just prior to the burn experiment.

Table 1. Key meteorological instruments deployed during experiment.

Platform/Instrument	Sensor Type/ Model	Variables	Measurement Height (m AGL)	Sampling Frequency
Meteorological tower (10 and 42 m)	3-D sonic anemometers (ATI, SAT-Sx; *RM Young 81000)	*u*, *v*, *w*, T_S	10 m and 6.0, 10.0, 20.0 & *42.0 for the 42 m tower	10 Hz
	Type-E, Fine-wire thermocouples	*T*	0 to top	1 Hz
	Total heat flux	kW m^{-2}	2.8	5 Hz
	Radiative heat flux	kW m^{-2}	2.7 (42 for 42 m tower)	5 Hz
CSU-MAPS 32 m portable tower	Thermistor/hygristors (Vaisala HMP45C)	*T*, *RH*	7.0-31.0	1 min
	3-D sonic anemometers (RM Young 81000)	*u*, *v*, *w*, T_S	7.0 & 31.0	10 Hz
Doppler mini SoDAR	Atmospheric Research & Technology, VT-1	*u*, *v*, *w*	15.0-200	10 min
Doppler SoDAR	Scintec MFAS-64	*u*,*v*,*w*	20-500	10 min
Doppler Lidar	Halo Photonics, Ltd., model Streamline 75	*u*, *v*, *backscatter*	0-1200	1 Hz
Microwave profiler	Radiometrics, Corp., MP-3000A	*T*, *RH*	0-10000	1 Hz
Weather balloon sounding system	GRAW Radiosondes, Gmb, GS-E	*T*,*RH*,*P*, *WS*,*WD*	0-15 km	1 Hz
Cup and Vane Anemometers	S-WCA-M003, Onset Computer Corporation	*WS/WD*	3.3	3 s
Temperature loggers	Onset, Inc, Hobo loggers,	*T*	0.0	1 Hz
Pressure Sensors	SJSU Custom	*T*, *p*	3.0	1 Hz

Table 2. Fuel moisture values (in percent) per sample type taken at the FireFlux II prairie.

Sample Type	Sample Size (n)	Mean (in %)	Median (in %)	Confidence Level (95%)	Standard Error	Standard Deviation
UL Grass	5	8.49	9.05	1.01	0.52	1.15
LL Grass	10	18.14	17.17	2.00	1.02	3.22
Forb	5	16.07	9.56	12.77	6.51	14.57

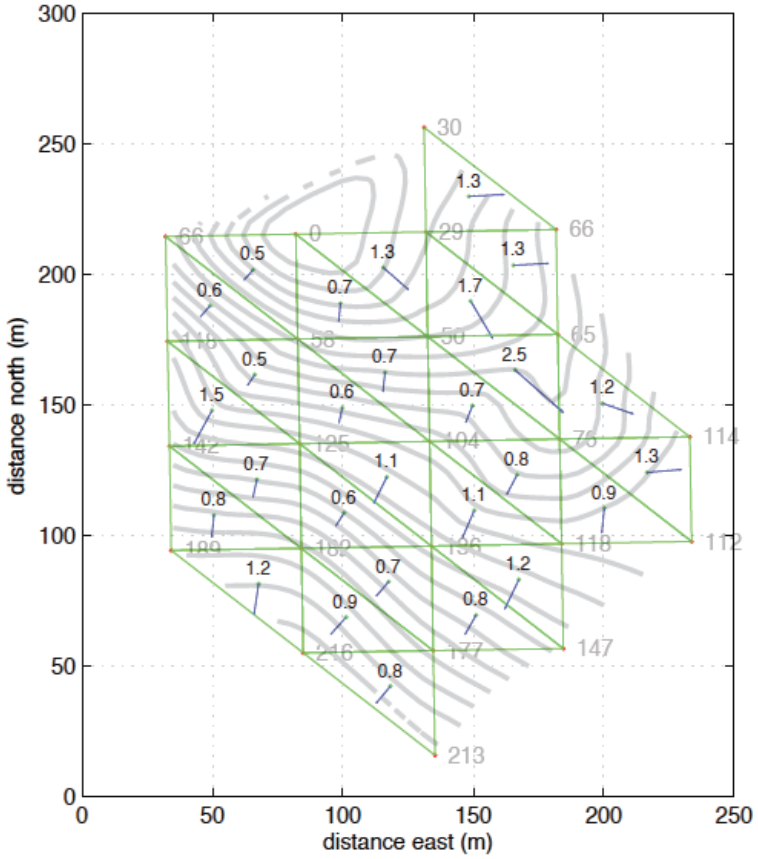

Figure 4. Rate of Spread vector calculation made from 28 ground thermocouples. Arrival times (s) at each HOBO, isochrones at 10-s intervals, ROS vectors, and ROS speed. (m/s).

3.3. In situ tower observations

Wind and temperature observations made from the 42 m tower are shown in Figure 5 for each measurement level. The time series shows little variability in the u-component wind, which is the streamwise component velocity, except for a slight decrease in velocity at the 20 m height just before the fire passes the tower. However, in the crosswind, v-component, the winds change from 2 m s-1 to nearly 6 m s-1 at 6 m AGL. Similar structure was observed at 10 m AGL, but not as large in magnitude (Figure 5). These observations indicate that the strongest fire-induced circulations occur at the surface near the fire front while above the fire, the ambient winds have a more pronounced effect on the plume, as indicated by the 20 m wind speed not changing from ambient. This fire-induced shear layer, where the surface winds accelerate and shift in direction at the fire front, can potentially increase turbulence generation near the surface potentially impacting fire behaviour.

The fire front passage is indicated by the sharp increase in temperature in Figure 5 (lowest panel) where maximum temperatures reached ~150 °C. At this same period, maxima in vertical velocities occurred at each level of the tower associated with the updraft of the plume. The maximum-recorded velocity was 8 m s^{-1} at the 20 m AGL level while at 10 m AGL the maximum updraft velocity was approximately 4 m s^{-1}.

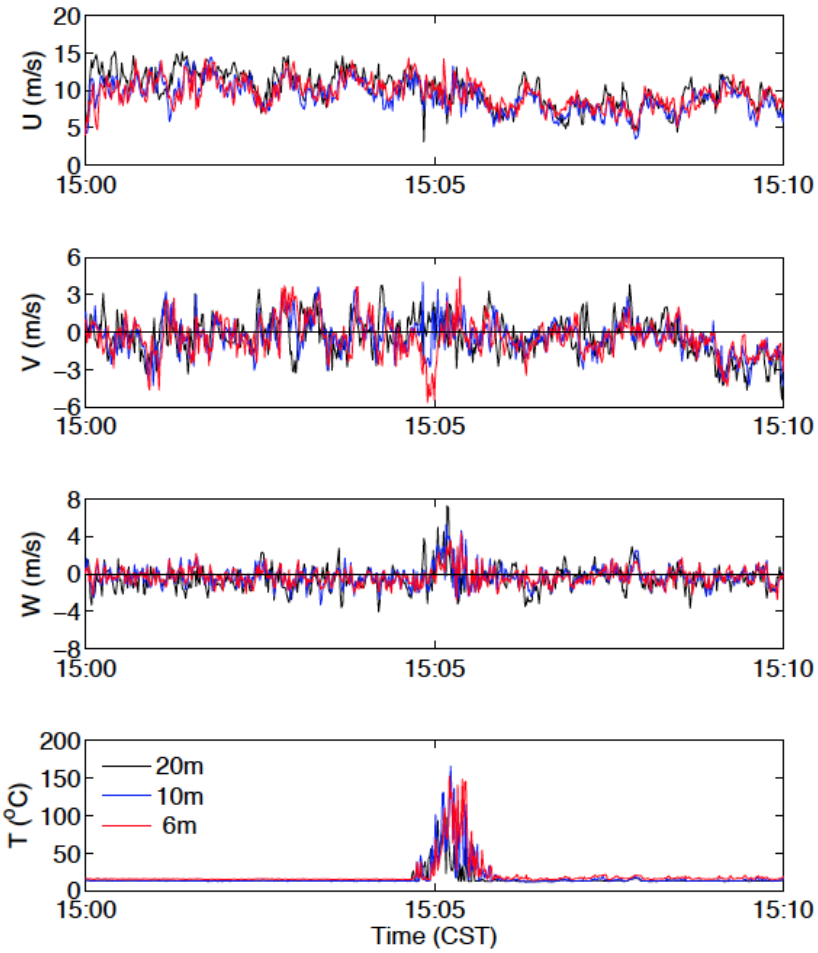

Figure 5. Time series of winds (u,v,w) and plume temperatures (T) during fire front passage (1505 CST) at the 42 m tower. Top panel is the u-component of velocity rotated into mean wind, v-componet is the cross-wise wind, w velocity is vertical component. Temperatures are taken from Sonic anemometers.

3.4. Photogrammetric analysis

For FireFlux II, photogrammetric analysis techniques were implemented in order to identify the fire spread rates for the head and flank fires. The technique, previously applied to fire front passage studies in controlled environments (Pastor et. al 2006), uses georectified high-definition and infrared imagery from a helicopter, correlated with georeferenced Plan Position Indicator (PPI) Doppler lidar scans, tower data, and perimeter anemometer plots, to create a comprehensive view of the wind field of the burn plot. In addition, georectifiying the helicopter high definition and infrared imagery to the prairie also allows for fire front tracing, providing an alternative method to calculating fire spread rates.
Preliminary photogrammetric analysis shows the progression of the fire as it burned across the prairie (Figure 6). Figure 6a, at ignition time, shows strong winds in excess of 10 m s-1 from 300 degrees, consistent with data from the perimeter anemometers, SoDARs, and tower data. Figure 6b, at approximately 86s after ignition, shows the development of the smoke plume moving with the wind

as the fire passes through the main tower, as seen by the black backscatter intensity contours. The smoke created by the backing fire along the edge of ignition also appears. Lidar data immediately downwind of the smoke plume contains errors, likely due to the lidar beam's inability to penetrate past the smoke. Figures 6c and 6d show the continued progress of the smoke plume over the prairie as the fire develops. Fire spread rate calculations using the georeferenced helicopter imagery shows a head fire spread rate of ~1.3-1.5 m s^{-1} and flank fire spread rate of ~0.5-0.7 m s^{-1}, which correlates well with the rate of spread calculations taken from the in ground temperature sensors (Figure 4). However, the error in this technique increased approximately 160 seconds into the burn, due to the change in the helicopter's altitude and angle in relation to the surface, skewing the error.

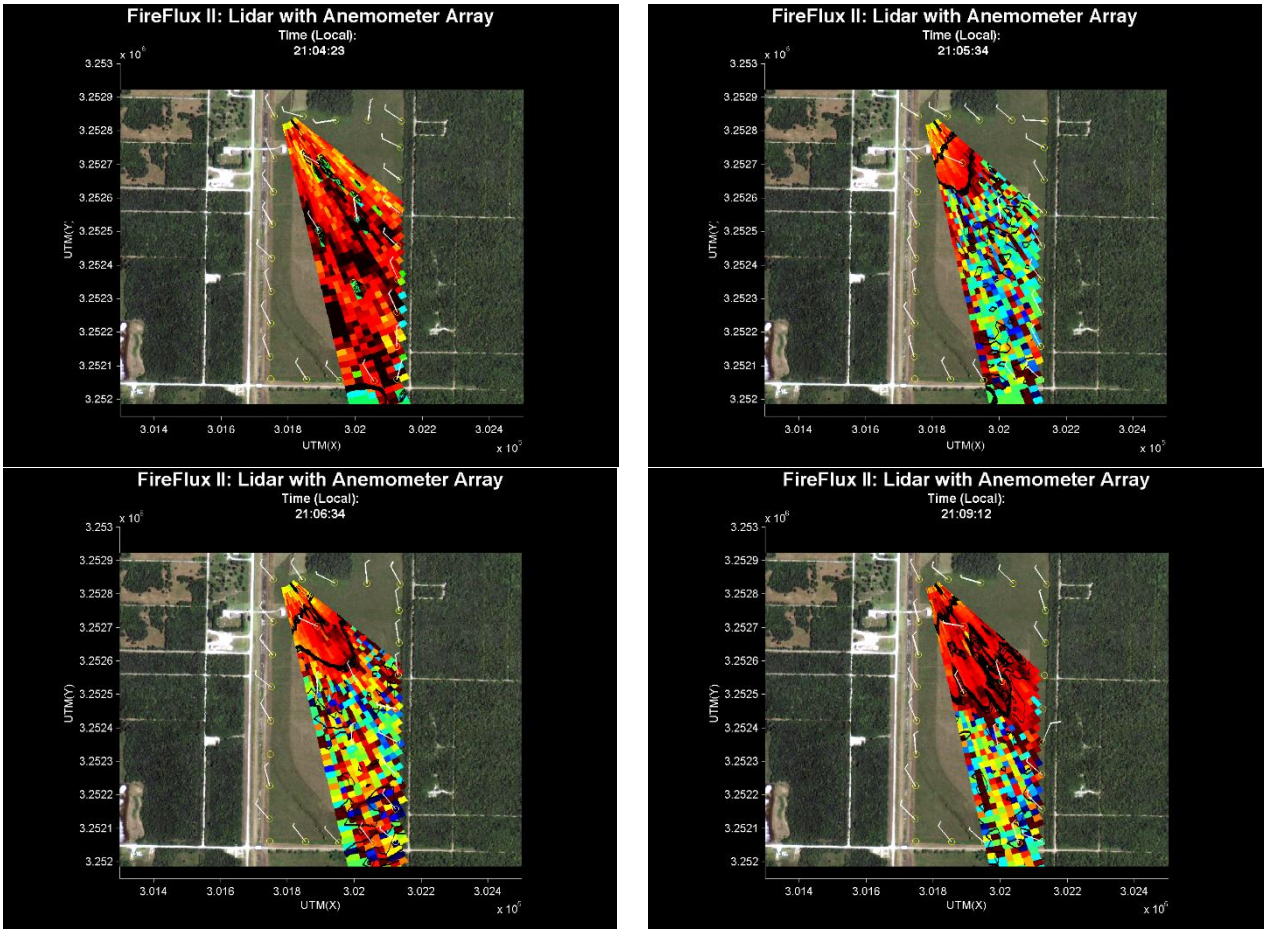

Figure 6. Time series of georectified images from FireFlux II, with Doppler lidar imagery superimposed over perimeter anemometer wind barbs. Black lines within the lidar scan designate the location of the smoke plume.

4. Conclusions

Analysis on the FireFlux II dataset is ongoing, and the work presented is a preliminary assessment of the potential for the data. The goal of improving upon the limitations of the original FireFlux field campaign is attained, as FireFlux II provides several methods for measuring fire spread rate and fire behaviour properties. Preliminary photogrammetric analysis gives a reliable method for calculating spread rate, coinciding well with values attained from ground thermocouple vector calculations. Future work in this area involves using the photogrammetric analysis method in the vertical, by correlating range height indicator (RHI) Doppler lidar scans to photography of the smoke plume, in order to further study the spread rate of the fire, as well as smoke plume dynamics. Data collected from pressure

sensors located within the experimental plot also shows promise in uncovering more information on pressure perturbations at the fire front.

Additionally, the FireFlux II dataset reinforces information gained in the original FireFlux campaign, providing more vertical wind and temperature measurements within the prairie with more in situ tower measurements. With these supporting datasets, we hope to build a more robust data library for model validation and more in depth fire-atmosphere interaction study.

5. Acknowledgements

This experiment would not have been possible without help and management from the following individuals and agencies. The Texas A & M Forest Service is thanked for conducting the burn operations. We want to thank the Rich Gray and his team for managing the burn operations, Dave Popoff from Galveston County Emergency Management for helping organizing county operations and personnel, Capt. Todd Weidman from La Margue Fire Dept for logistics and providing his staff of fire fighters, Prof. Steve Pennings and Tim Becker of the University of Houston Coastal Center for the research permit and help with all the logistics at the site, Paul Sopko (USFS), Ben Hornsby (USFS), Joe Restaino (USFS), and Dianne Hall (SJSU) for help with field sampling and setup, and Kent Prochazka (NWS Houston) for the fire weather forecasts. This research was funded by grants from the National Science Foundation (AGS-1151930) and Joint Fire Science Program (#11-2-1-11).

6. References

Cheney NP, Gould JS, Catchpole WR, 1998: Prediction of fire spread in grasslands. Int J Wildland Fire 8:1-13

Clark, T. L., Jenkins, M. A., Coen, J., Packham, D., 1996: A coupled atmosphere-fire model: Convective feedback on fire-line dynamics. J. Appl. Meteorol. 35, 875-901.

Clements C B et al., 2007: Observing the dynamics of wildland grass fires: FireFlux – a field validation experiment. B Am Meteorol Soc 88:1369–1382

Clements C B et al., 2008: First observations of turbulence generated by grass fires, J. Geophys. Res., 113, D22102, doi:10.1029/2008JD010014.

Filippi J B, Pialat X, Clements C B, 2013: Assessment of FOREFIRE/MESONH for wildland fire/atmosphere coupled simulation of the FireFlux experiment. P Combust Ins: 2633- 2640

Kochanski A K, Jenkins M A, Mandel J, Beezley J D, Clements C B and Krueger S, 2013: Evaluation of WRF-SFIRE performance with field observations from the FireFlux experiment. Geo Model Devel 6:1109-1126

Linn, R. R., and P. Cunningham, 2005: Numerical simulations of grass fires using a coupled atmosphere-fire model: Basic fire behavior and dependence on wind speed. J. Geophys. Res., 110, D13107, doi:10.1029/ 2004JD005597

Mandel J, Beezley, J D, and Kochanski, A K: Coupled atmosphere-wildland fire modeling with WRF 3.3 and SFIRE, Geosci. Model Dev., 4, 591–610, doi:10.5194/gmd-4-591-2011.

Mell, W, Jenkins M, Gould J, Cheney P, 2007: A physics-based approach to modelling grassland fires. Int J Wildland Fire 16:1–22

Pastor, E., et al., 2006: Computing the rate of spread of linear flame fronts by thermal image processing, Fire Safety Journal, Volume 41, Issue 8, Pages 569-579, ISSN 0379-7112.